Hindawi Publishing Corporation
EURASIP Journal on Wireless Communications and Networking
Volume 2009, Article ID 682368, 12 pages
doi:10.1155/2009/682368

Research Article

Spatial and Temporal Fairness in Heterogeneous HSDPA-Enabled UMTS Networks

Andreas Mäder[1] and Dirk Staehle[2]

[1] *Department of Distributed Systems, University of Wuerzburg, Sanderring 2, 97070 Würzburg, Germany*
[2] *NEC Laboratories Europe, Kurfuersten-Anlage 36, 69115 Heidelberg, Germany*

Correspondence should be addressed to Andreas Mäder, maeder@informatik.uni-wuerzburg.de

Received 15 July 2008; Revised 27 November 2008; Accepted 29 December 2008

Recommended by Ekram Hossain

The system performance of an integrated UMTS network with both High-Speed Downlink Packet Access users and Release '99 QoS users depends on many factors like user location, number of users, interference, multipath propagation profile, and radio resource sharing schemes. Additionally, the user behavior is an important factor; users of Internet best-effort applications tend to follow a volume-based behavior, meaning they stay in the system until the requested data is completely transmitted. In conjunction with the opportunistic transmission scheme implemented in HSDPA, this has implications to the spatial distribution of active users as well as to the time-average user and cell throughput. We investigate the relation between throughput, volume-based user behavior and traffic dynamics with a simulation framework which allows the efficient modeling of large UMTS networks with both HSDPA and Release '99 users. The framework comprises an HSDPA MAC/physical layer abstraction model and takes network aspects like radio resource sharing and other-cell interference into account.

1. Introduction

Mobile network operators continue to deploy the High-Speed Downlink Packet Access (HSDPA) service in their existing Universal Mobile Telecommunication System (UMTS) networks. From the users perspective, the HSDPA promises high data rates (up to 14.4 Mbps with Release 5) and low latency. From the perspective of an operator, HSDPA is hoped to play a key role for the much longed for breakthrough of high-quality mobile data services. From a technical perspective, HSDPA introduces a new paradigm to UMTS; instead of adapting the transmit power to the radio channel condition in order to ensure constant link quality, HSDPA adapts the link quality to the radio channel conditions. This enables a more efficient use of scarce resources like transmit power, channelization codes, and also hardware components.

The basic principle of the HSDPA is to adapt the link to the instantaneous radio channel condition using adaptive modulation and coding (AMC). HSDPA employs a shared channel, the High-Speed Downlink Shared channel (HS-DSCH), which is used by all HSDPA users. With a shared channel, radio resources are occupied only if a transmission occurs, which enables a more efficient transport of bursty traffic. In each transport time interval (TTI), the scheduler located in the NodeB decides about the users to be scheduled and about their data rate. The scheduling decision can be either on behalf of channel quality indicator (CQI) reports from the user equipments (UE) to enable opportunistic scheduling schemes which use the air interface more efficiently, or simple nonopportunistic schemes like round-robin can be used which shares the resources time fair among the users.

An important aspect of HSDPA systems is the perceived fairness of the connection metrics between the users. This is in contrast to pure UMTS Release '99, where the circuit-switched design of the radio bearers guarantees equal Quality of Service (QoS) properties of all users of the same service class [1]. However, since in HSDPA the theoretically achievable data rate depends on the channel condition, the actual achieved data rates depend on user location, number of users, interference, scheduling discipline, and in

integrated networks also on the number of dedicated channel (DCH) connections. In this work, we distinguish between two fairness aspects. *Spatial fairness* refers to the spatial distribution of the perceived data rates within a cell or sector. *Temporal fairness* refers to the long-term time-average user throughput [2].

Our contribution is twofold: first, we propose a flow-level simulation framework which takes on the one hand physical layer aspects, scheduling disciplines, interference, and radio resource management schemes into account, but also allows for simulation of large networks due to its analytical approach. Second, we investigate the impact of three well-known scheduling disciplines, namely round-robin, proportional fair, and Max C/I on the spatial user distribution and on the system and user performance. One of our main findings is that Max C/I scheduling, although providing sum-rate optimal rate allocations in *static* system scenarios, performs worse than proportional fair scheduling if traffic dynamics are considered.

The remaining of this article is organized as follows: in the next section, we motivate our work and give an overview of the current literature. In Section 3, we give a brief overview of the HSDPA. In Section 4, we explain radio resource sharing between DCH and HSDPA connections and formulate a model for the calculation of NodeB transmit powers. In Section 6, a physical layer abstraction model for the HSDPA is proposed which enables the calculation of the average throughputs per flow for different scheduling disciplines. Simulation scenarios and numerical results are presented in Section 7, followed by a conclusion in Section 8.

2. Motivation and Related Work

The focus of this work is the impact of elastic flows on the system performance. We have to distinguish between QoS flows which require a fixed bandwidth, as for voice calls over DCH transport channels, and "best-effort" or elastic flows which adapt their bandwidth requirements to the currently available bandwidth. Such a flow may be an FTP transfer or the combined elements of a web page including inline objects such as embedded videos, that may be transmitted in parallel TCP connections. A flow can be loosely defined as a coherent stream of data packets with the same destination address [3]. An important distinction between the two types of flows is that QoS flows typically follow a time-based traffic model, which means that the user wants to keep the connection for a certain time span. In contrast, elastic flows are volume-based, that is, the user is satisfied as soon as a certain data volume is transmitted. An effect in this context which is that of *spatial inhomogeneity*, which has been mentioned in [4] for systems without AMC, and has been further investigated in [5, 6] for pure single-cell HSDPA systems. Users with bad radio conditions experience lower data rates than users with better radio conditions, leading to a spatial unfairness, which we define as the discrepancy between location-dependent user arrival probabilities and the observed residence probabilities in steady state. We investigate this effect in Section 7.1 for different scheduling disciplines in a multicell scenario, that is, with consideration of other-cell interference, and with location-dependent arrival rates.

A related point is the system performance and fairness of the perceived data rates under different scheduling regimes. In the literature, a large number of fundamental works investigate the tradeoff between fairness and system capacity in a wireless systems with opportunistic scheduling. Examples can be found in [2, 7–10], where in [7] the concept of multiuser diversity (MUD) in downlink direction has been investigated, motivated by the findings in [11] for the uplink direction. For HSDPA systems, research mainly concentrated on variations of the proportional fair scheduler developed for the 1xEV-DO system [12]. Different approaches exist to include QoS constraints on delay or data rate into the scheduling decision [13–17]. The fairness of different schedulers in HSDPA systems is investigated in [18, 19]. Both works conclude that Max C/I provides the highest system throughput. We compare user and system throughput for round-robin, Max C/I, and proportional fair scheduling. The results show that on the one hand, as expected the two channel-aware schemes clearly outperform round-robin scheduling, but on the other hand, proportional fair scheduling leads to a higher time-average throughput than Max C/I scheduling. We discuss this result in detail in Section 7.2.

Statistically valid results for integrated UMTS networks require long simulation runs or analytical approaches. An intuitive example is the DCH blocking probability; a DCH user which is located far from the antenna is subject to strong interference from surrounding NodeBs, he may therefore require a very high transmit power. If this user additionally has a long call time, the influence on the blocking probability is significant. Since such events occur not very often with reasonable loads, long simulation runs are required. The results in this work are therefore generated with a simulation framework based on [20, 21], that uses analytic methods to approximate the effects of the physical layer and the scheduling discipline on flow level. This allows for accurate and time-efficient simulations of large UMTS networks.

3. System Description

We consider a UMTS network where HSDPA and DCH connections share the same radio resources, namely transmit power and channelization codes. The core of the HSDPA is the HS-DSCH, which uses up to 15 codes with spreading factor (SF) 16 in parallel. The HS-DSCH enables two types of multiplexing; time multiplex by scheduling the subframes to different users, and code multiplex by assigning each user a nonoverlapping subset of the available codes. The latter requires the configuration of additional High-Speed Shared Control Channels (HS-SCCHs). Throughout this work we assume that only one HS-SCCH is present, hence consider time multiplex only.

In contrast to dedicated channels, where the transmit power is adapted to the propagation loss with fast power control and thus enabling a more or less constant bit rate, the HS-DSCH adapts the channel to the propagation loss

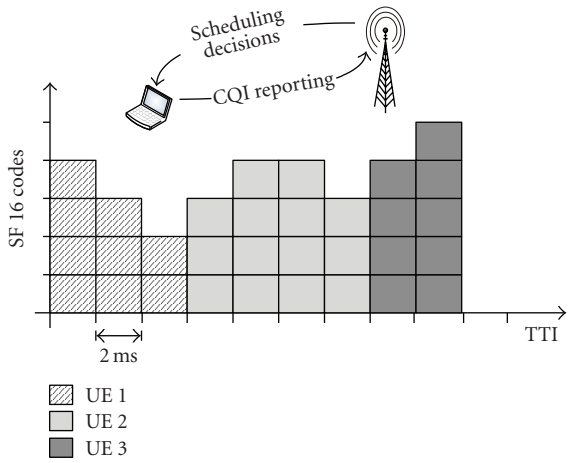

Figure 1: Schematic view of the HSDPA transport channel.

with AMC. The UE sends CQI values to the NodeB. The CQI is a discretization of the received signal-to-interference ratio (SIR) at the UE and ranges from 0 (no transmission possible) to 30 (best quality). The scheduler in the NodeB then chooses a transport format combination (TFC) such that a predefined target BLER, which is often chosen as 10%, is fullfilled if possible. The TFC contains information about the modulation (QPSK or 16QAM), the number of used codes (from 1 to 15), and the coding rate resulting in a certain transport block size (TBS) that defines the information bits transmitted during a TTI. A number of tables in [22] define a unique mapping between CQI and TFC. This means that with an increasing CQI, the demand on code resources is also increasing. This leads to cases where a high CQI is reported to the NodeB, but the scheduler has to select a lower TBS due to lacking code resources. A schematic view of the HSDPA functionality is shown in Figure 1.

4. Sharing Code and Power Resources between HSDPA and DCH

A key issue of the radio resource management in HSDPA enhanced UMTS networks is the sharing of code and power resources between DCHs, signaling channels, common channels, and finally channels required for the HSDPA, namely, the HS-DSCH and the HS-SCCH. The signaling channels and common channels mostly require a fixed channelization code and a fixed power as for the pilot channel (CPICH) or the forward access channel (FACH). The DCHs are subject to fast power control which means that their power consumption depends on the cell or system load that determines the interference at the UE. The general level of power consumption depends on the processing gain and the required target bit-energy-to-noise ratio (E_b/N_0) of the radio access bearer (RAB).

The HSDPA requires code and power resources. Codes are the channelization codes that are generated according to the orthogonal variable spreading factor (OVSF) code tree. The number of codes that is available for a certain spreading factor (SF) is equal to the spreading factor itself. A 384 kbps DCH occupies an SF 8 channelization code. Accordingly, the maximum number of parallel 384 kbps users per sector is theoretically 8. In practice, only 7 parallel 384 kbps users are possible since the signaling and common channels also require some code resources. Let us introduce an SF 512 code as the basic code unit. Then, a DCH i with SF k occupies $c_i = 512/k$ code resources. An HSDPA code with SF 16 requires $c_{\text{HS}} = 32$ code resources. Let C_{DCH} be the total code resources occupied by all DCHs, C_{CCH} be the resources occupied by signaling and common channels, and, $C_{\text{HS}} = n_{\text{HS}} \cdot c_{\text{HS}}$ be the total number of code resources used by the HSDPA where n_{HS} is the number of SF 16 codes allocated to the HS-DSCH. The total number of code resources is equal to $C_{\text{tot}} = 512$. We consider *adaptive* code allocation [23, 24], which is illustrated in a simplified view (pilot and control channels are omitted) in Figure 2 for both transmit power and channelization codes. We further assume that the codes are always optimally arranged in the code tree, and that no code tree fragmentation occurs. The number of codes available for the HSDPA is then

$$n_{\text{HS}} = \left\lfloor \frac{C_{\text{tot}} - C_{\text{CCH}} - C_{\text{DCH}}}{c_{\text{HS}}} \right\rfloor. \tag{1}$$

Accordingly, the transmit power $T_{x,\text{tot}}$ consists of a constant part T_{CCH} for common and signaling channels, a part T_{DCH} for DCHs, and a part T_{HS} for the HS-DSCH. Let T^* be the target transmit power at the NodeB. Then, the HS-DSCH power with adaptive power allocation is

$$T_{\text{HS}} = T^* - T_{\text{CCH}} - \overline{T}_{\text{DCH}}, \tag{2}$$

where T^*_{HS} is the power reserved for the HS-DSCH, and $\overline{T}_{\text{DCH}}$ is the total DCH power averaged over some period of time.

5. Calculation of Downlink Transmit Powers

We define a UMTS network as a set $\mathcal{L}$ of NodeBs with associated UEs, $\mathcal{M}_x$. A DCH connection k corresponds to a radio bearer at NodeB $x \in \mathcal{L}$ with data rate R_k and code resource requirements c_k. Since the power consumed by the DCH connection is subject to power control, the received E_b/N_0 ε_k fluctuates around a target-E_b/N_0 value $\overline{\varepsilon}^*_k$, which is adjusted by the outer-loop power control such that the negotiated QoS parameters like frame error rate are fulfilled. A common approximation for the average E_b/N_0 value is

$$\overline{\varepsilon}_k = \frac{W}{R_k} \cdot \frac{T_{k,x} \cdot d_{k,x}}{W \cdot N_0 + I_{k,\text{oc}} + \alpha_i \cdot T_{x,\text{tot}} \cdot d_{k,x}}, \tag{3}$$

where the orthogonality α_k describes the impact of the multipath profile for DCH k, $d_{k,x}$ is the average path gain between NodeB x and UE k, W is the system chip rate, and N_0 is the thermal noise density. We assume perfect power control, that is, the mean E_b/N_0 value meets exactly the target-E_b/N_0 such that $\overline{\varepsilon}_k = \overline{\varepsilon}^*_k$. The mean transmit power requirement of a DCH connection follows then as

$$T_{k,x} = \frac{\overline{\varepsilon}^*_k \cdot R_k}{W} \cdot \left(\frac{W \cdot N_0 + I_{k,\text{oc}}}{d_{k,x}} + \alpha_k \cdot T_{x,\text{tot}} \right). \tag{4}$$

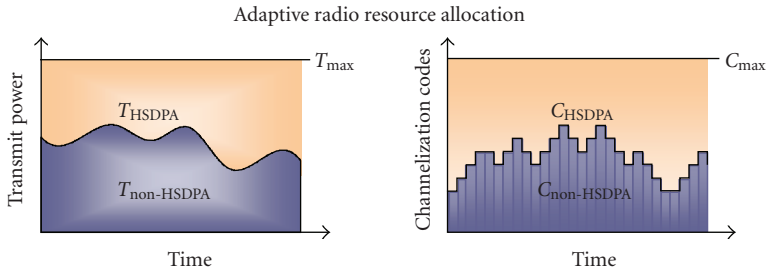

Figure 2: Adaptive radio resource management scheme.

The average other-cell interference comprises the received powers of surrounding NodeBs such that $I_{k,\mathrm{oc}} = \sum_{y\in\mathcal{L}\setminus x} T_{y,\mathrm{tot}} \cdot d_{k,y}$. The total NodeB transmit powers can be calculated with an equation system over all NodeBs. For that reason, we follow [25] and define the load of NodeB x with respect to NodeB y as

$$\eta_{x,y} = \sum_{k\in\mathcal{M}_x} \omega_{k,y},$$
$$\text{with } \omega_{k,y} = \frac{\overline{\varepsilon}_k^* \cdot R_k}{W} \cdot \begin{cases} \alpha, & \text{if } \mathcal{L}(k) = y, \\ \dfrac{d_{k,y}}{d_{\mathcal{L}(k),k}}, & \text{if } \mathcal{L}(k) \neq y. \end{cases} \tag{5}$$

After some algebraic modifications, this allows us to formulate the total DCH transmit power in a compact form as

$$T_{x,\mathrm{DCH}} = \sum_{y\in\mathcal{L}} \eta_{x,y} \cdot T_{y,\mathrm{tot}}. \tag{6}$$

In this equation, we neglect the thermal noise since in a reasonable designed network its impact on the transmit power requirements is minimal. Note also that the equation includes the case $y = x$ for the own-cell interference. For the total transmit power we introduce the boolean variable $\delta_{y,\mathrm{HS}}$ indicating whether at least one HSDPA flow is active in cell x. The total transmit power at NodeB x is then

$$T_{x,\mathrm{tot}} = \delta_{x,\mathrm{HS}} \cdot T_x^* + (1 - \delta_{x,\mathrm{HS}}) \cdot \left(T_{x,\mathrm{CCH}} + \sum_{y\in\mathcal{L}} \eta_{x,y} \cdot T_{y,\mathrm{tot}}\right). \tag{7}$$

This equation states that if the HS-DSCH is active, the total transmit power is equal to the target power. Otherwise, it consist only of the DCH transmit power and the transmit power for common channels. Introducing the vectors

$$V[x] = \delta_{x,\mathrm{HS}} \cdot T_x^* + (1 - \delta_{x,\mathrm{HS}}) \cdot T_{x,\mathrm{CCH}}, \tag{8}$$

and matrix

$$M[x,y] = (1 - \delta_{x,\mathrm{HS}}) \cdot \eta_{x,y} \tag{9}$$

leads to the matrix equation

$$T = V + M \cdot T \Longleftrightarrow T = (I - M)^{-1} \cdot V, \tag{10}$$

which provides the transmit powers of all NodeBs in the system. The matrix I is the identity matrix, and T is the vector of NodeB transmit powers T_x. The DCH and HSDPA transmit powers are then calculated with (6) and (2).

6. HSDPA Physical Layer Model

Consider an HS-DSCH with power $T_{\mathrm{HS}} = \Delta_{\mathrm{HS}} \cdot T_{\mathrm{tot}}$ and n_{HS} parallel codes allocated to the HS-DSCH. Accordingly, the SIR at UE i for a RAKE receiver with perfect maximum ratio combining is equal to

$$\gamma_i = \Delta_{\mathrm{HS}} \cdot \sum_{p\in\mathcal{P}} \frac{T_{\mathrm{tot}} \cdot d_{i,p,x}}{W \cdot N_0 + I_{\mathrm{oc},i} + \sum_{r\in\mathcal{P}\setminus p} T_{x,\mathrm{tot}} \cdot d_{i,r,x}}, \tag{11}$$

where $d_{i,p,x}$ is the instantaneous propagation gain of signal path $p \in \mathcal{P}$. The UE measures the SIR and maps it to the maximum CQI with a transmission format that achieves a frame error rate of 10%. In [26] the following relation of SIR and CQI q is given:

$$q = \max\left(0, \min\left(30, \left\lfloor \frac{\mathrm{SIR[dB]}}{1.02} + 16.62 \right\rfloor\right)\right). \tag{12}$$

The CQI-value q defines the maximum possible TBS $v(q)$, that can be transmitted in one TTI. It also defines the number of required parallel codes $n_{\mathrm{HS}}(q)$. If the number of available codes n_{HS} is less than $n_{\mathrm{HS}}(q)$, the scheduler selects the maximum possible TBS value according to n_{HS}. This means that an optimal usage of resources is only possible if the transmission format according to the reported CQI utilizes all available codes. If too few code resources are available, power resources are wasted, and if too few power resources are available, the CQI is too small to utilize all available codes. The reported CQI value depends essentially on the multipath profile, the users' location, the available HS-DSCH power, and the other-cell power. The number of codes required for a certain CQI value depends on the CQI category.

Above equations give the CQI and TBS for a concrete instance of the propagation gains in particular of the multipath component power. For a simplified simulation and evaluation of the HSDPA performance, an approximate model for the HSDPA bandwidth similar to the orthogonality factor model for DCH is required. The orthogonality factor [27] is used to determine the signal-to-interference ratio for a DCH i as

$$\gamma_i = \frac{W}{R_i} \cdot \frac{T_x \cdot d_{x,i}}{I_{i,\mathrm{other}} + \alpha \cdot I_{i,\mathrm{own}}}, \tag{13}$$

where W/R_k is the processing gain, $I_{i,\mathrm{other}}$ is the other-cell interference, and $I_{i,\mathrm{own}} = T_{x,\mathrm{tot}} \cdot d_{x,i}$ is the own-cell

interference. The orthogonality factor α specifies the part of the power received from the own cell that contributes to the interference due to multipath propagation. It captures the impact of the multipath profile in a single value between 0.05 and 0.4 depending on the multipath profile. For a deeper discussion of the orthogonality factor model please refer to [28–30] and the references therein.

Actually, the values γ_k, I_{own}, and I_{other} are mean values averaged over the short-term fading. More precisely, we should write (13) as

$$E[\gamma_i] = \frac{W}{R_i} \cdot \frac{T_{x,i} \cdot d_{x,i}}{E[I_{i,\text{other}}] + \alpha \cdot E[I_{i,\text{own}}]} = \frac{W}{R_i} \cdot \frac{T_{x,i}}{T_{x,\text{tot}}} \cdot \frac{1}{E[I_{i,\text{other}}]/E[I_{i,\text{own}}] + \alpha}. \tag{14}$$

The orthogonality factor model is not applicable to the HSDPA since it only yields the mean SIR. However, for the evaluation of the average HSDPA data rate of a UE at a certain location, the distribution of the reported CQI values is required. The essential assumption of the orthogonality factor model is that the mean normalized SIR, that is, the last fraction in (14), is a function of the ratio Σ of average other-cell received power and average own-cell received power (or short other-to-own-cell power ratio)

$$\Sigma_i = \frac{E[I_{i,\text{other}}]}{E[I_{i,\text{own}}]} = \frac{\sum_{y \neq x} T_{y,\text{tot}} \cdot d_{y,i}}{T_{x,\text{tot}} \cdot d_{x,i}}. \tag{15}$$

In [20], the orthogonality factor model is enhanced to yield not only the mean but also the standard deviation of the SIR in decibel scale as a function of Σ_i. Assuming that the distribution of the SIR follows a normal distribution that is entirely characterized by its mean and standard deviation, the distribution of the reported CQI values, $p_{\text{CQI}}(q)$, is obtained from the cumulative density function (CDF) of the distribution of the SIR. Truncating the CQI distribution according to the available codes for the HS-DSCH yields the distribution of the TBS as

$$p_{\text{TBS}}(v) = \begin{cases} p_{\text{CQI}}(v(q)), & \text{if } v(q) < v^*, \\ \sum_{q=v^*}^{30} p_{\text{CQI}}(q), & \text{else}, \end{cases} \tag{16}$$

where v^* is the maximum allowed TBS according to the available code resources. Accordingly, we denote the CDF of the CQI and TBS values with $P_{\text{CQI}}(q)$ and $P_{\text{TBS}}(v)$.

The physical layer abstraction model gives also insights into the impact of system parameters like multipath channel profile, number of available codes and, UE category. Figure 3 shows the gross data rate, that is, the throughput a single UE would achieve, depending on the other-to-own-interference ratio for the ITU Vehicular A, Pedestrian A, and Vehicular B multipath propagation models. A profile with a strong dominating path, like in Pedestrian A, enables indeed very high data rates up to 13 Mbps. In contrast, profiles with a relatively strong second path, like Vehicular A and Vehicular B, lead to significantly lower data rates due to a higher

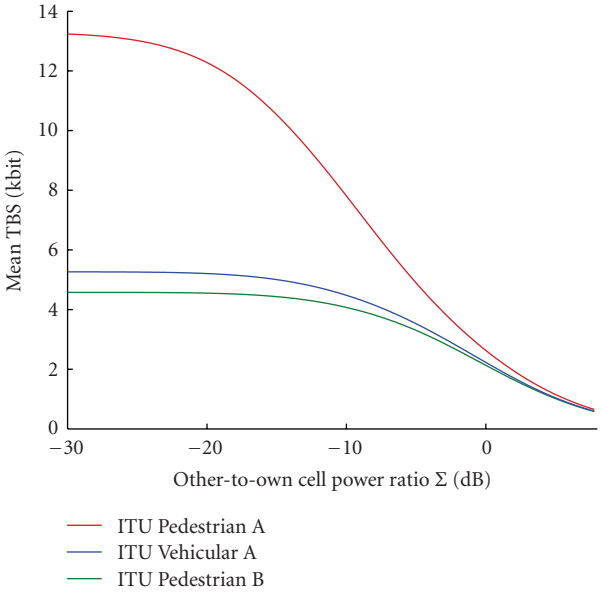

Figure 3: Gross data rate for different channel profiles.

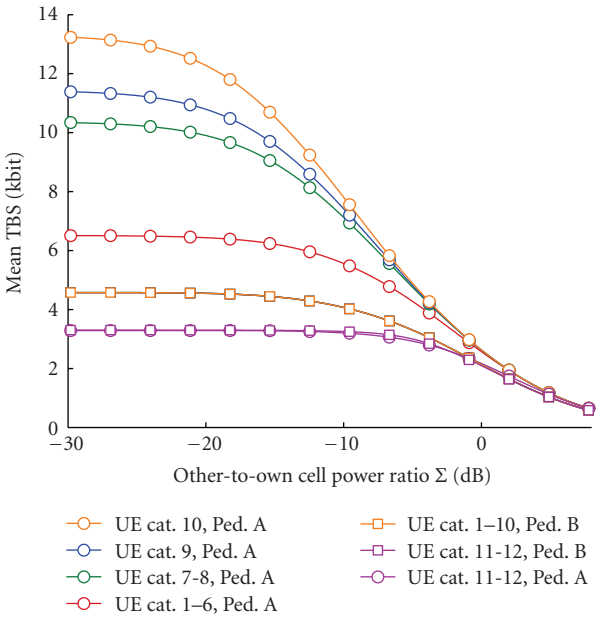

Figure 4: Gross data rates for different UE categories.

intersymbol interference. In fact, with these two models, it is sufficient to provide five SF 16 codes for the HS-DSCH. Figure 4 shows the gross data rates for different UE categories, which reflect the capability for 16QAM, number of parallel codes and, interscheduling time. Interesting is that UEs without QAM 16 support (categories 11 and 12) have significantly lower data rates than UEs with QAM 16, although the transport block sizes are identically (categories 1–6).

6.1. Scheduling. The scheduler in the NodeB has a large influence on the user-level and system-level performance of

the HSDPA. Several proposals exist for HSDPA scheduling, from which we considered three of the most common schemes. The channel-blind round-robin scheme selects users consecutively for transmission. The MaxTBS-scheduler chooses always the user with the currently best possible TBS, including restrictions due to code resources. Finally, the proportional fair scheduler selects the user which has the proportionally best TBS in relation to its past throughput.

Channel-aware schedulers like MaxTBS and proportional fair benefit from multiuser diversity [7]. With an increasing number of users in a cell, the probability to see at least one user with good radio conditions also increases. If "strong" users are favored by the scheduler, the aggregated cell throughput increases. Exploitation of multiuser diversity is therefore in the end beneficial for the overall system capacity, also because reduced transmission times for volume-based users leads to longer time periods where the HS-DSCH is switched off—which in turn reduces interference.

6.1.1. Round-Robin Scheduling. The *round-robin* scheduler selects the users consecutively for transmission. In a sufficiently long time interval, the probability that a user k is selected is therefore approximately $1/|\mathcal{M}|$. Round-robin is a channel-blind scheduling discipline, which means that the average throughput of each mobile depends only on its channel condition and the number of users in the cell, but not on the channel conditions of other users. Consequently, the cell throughput does not benefit from multiuser diversity. However, round-robin is robust and does not suffer from any convergence issues like proportional fair scheduling in some cases [31], and it is easy to implement due to its simple principle. Round-robin is an allocation-fair scheduling discipline in the sense that, to every user, the same amount of radio resources in terms of codes and power are allocated. This approach is often sufficient to prevent starvation of users at the cell edge.

6.1.2. MaxTBS Scheduling. With *MaxTBS* (or Max C/I) scheduling, the user with the currently best TBS is scheduled. This scheduling discipline maximizes the sum-rate capacity (in our context the cell throughput) given the saturated case, that is, all users have at least one packet to transmit [32, 33]. If two or more users have the maximum possible TBS, a random user out of this set is selected with equal probability. In contrast to round-robin scheduling, the throughput of a user depends not only on its own location, but also on the location of the other users. In [6], this scheduling discipline is modeled as a priority queue, where locations closer to the NodeB have higher priority than locations farther away. However, it is also possible to calculate the average throughput directly from the TBS distributions of the users. In this work we use the formulation we developed in [21]. MaxTBS strongly favors the user with the best channel quality. This implicates that users with weak radio conditions are penalized and perceive on average very low data rates, leading to unfair rate allocations. We show in the next section how this behavior negatively affects the average throughput if traffic dynamics are considered.

6.1.3. Proportional Fair Scheduling. *Proportional fair* (PF) scheduling is a scheduling discipline which has been developed for the 1xEv-DO-system in the downlink [12]. The basic principle is to allocate each user proportional to its link quality and its past throughput. This is achieved by selecting the user that has the best instantaneous relative throughput over its past throughput, which is often calculated with a sliding window approach. However, different versions of PF scheduling exist. The most fundamental difference is the way how the past throughput is calculated. The first variant updates the past throughput every scheduling period regardless whether the user has been scheduled or not, the second variant updates the past throughput only if the user is indeed chosen for transmission. The difference between both versions is that in the first case the mean throughput of a user is proportional to its channel quality only, while in the second case it is also related to the generated traffic. In [31, 34] it is argued that both variants approximately lead to the same results in case of statistically identical fades and infinite backlogs. The second assumption is reasonable during the interevent time, while the first assumption is contradicted by the fact that the shape of the CQI distribution depends on the level of received other-cell interference. A direct formulation of the flow-average throughput and a comparison between both variants can be found in [21].

7. Flow-Level Performance Results

UMTS networks are dynamic systems because of the mutual dependency among the transmit powers of different cells. This means that a well-designed performance evaluation has to consider networks with a reasonable size in order to capture these effects and their impact on flow-level performance properly. We consider two different types of networks: a 19-NodeB hexagonal layout with a NodeB distance of 1.2 km, and an irregular layout with 22 NodeBs which is generated from a Voronoi tessellation. The network areas are partitioned into area elements with an edge length of 25 m. Figure 5 shows the irregular network with antenna locations (dots) and arrival cluster centers (stars). In the hexagonal layout, user arrive according to a homogeneous Poisson process such that arrival rates are equal for all area elements. In the irregular network, users arrive according to a clustered Poisson process as described in [25] and shown in Figure 6; the total arrival rate λ_f in an area element f results from the superposition of circular clusters with constant arrival rates. In the irregular network therefore not only the layout but also the arrival process is heterogeneous.

Results are generated with a time-dynamic simulation which considers the HSDPA data traffic of a user as a flow with a certain data volume. The network area is discretized into a set of area elements with an edge length of 25 m. The time axis is divided in interevent times. We assume that between two events the users stay roughly within an area element.

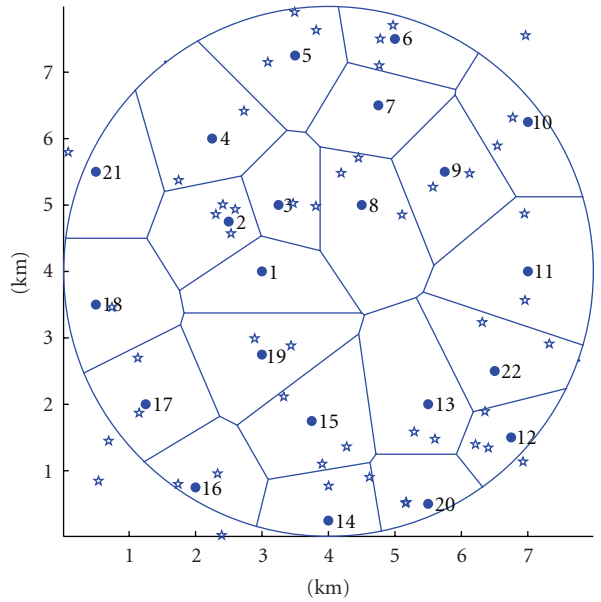

Figure 5: Irregular network layout. Dots indicate NodeB (antenna) locations, stars mark cluster centers.

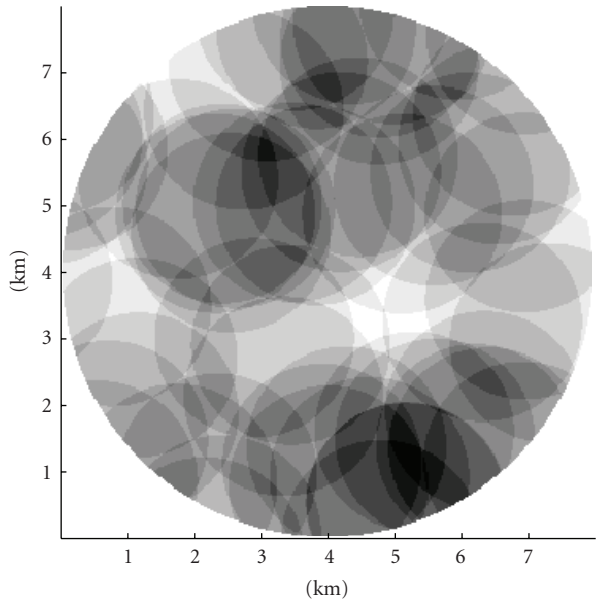

Figure 6: Inhomogeneous arrival densities. Darker colors indicate higher probability of arrival.

We consider two types of events: arrival events, that is, the arrival of a new user into the system, and departure events, which may occur if an HSDPA user has received all its data or if the call time of DCH user is reached. On arrival of a new user, admission control for DCH and HSDPA is performed. The admission control for DCH connections is threshold-based. An incoming connection is blocked if the total transmit power including the new connection exceeds the target transmit power, or if the available code resources are not sufficient. For this purpose, the required transmit power is calculated at the serving NodeB under the worst-case assumption that all NodeBs transmit with the target power in order to prevent possible outage. For the HSDPA, we assume a count-based admission control which restricts the maximum number of concurrent connections to a fixed value. If the incoming connection is admitted into the system, the call time or the data volume, depending on the user type, is calculated according to the respective distribution parameters. We assume exponentially distributed call times with mean $E[T] = 120$ s for DCH users and exponentially distributed flow sizes with mean volume $E[V] = 100$ KB for HSDPA users. The arrival rate of the DCH users is determined from the offered DCH code load defined as

$$\rho_c = \sum_{s \in \mathcal{S}} \frac{\lambda_s}{\mu_s} \cdot \frac{c_s}{C_{\text{tot}}}, \tag{17}$$

where $\mu_s = 1/E[T_s]$, and the index s denotes the service class of the radio bearer.

On each event, the system variables are recalculated if necessary. If the event is generated by a DCH arrival or departure, HSDPA code resources in the relevant cells are decreased or increased according to the DCH code requirements. Additionally, the total transmit powers are updated for all NodeBs in order to capture the new interference situation. Transmit power recalculation is also done if the HS-DSCH is switched on or off because of HSDPA user arrivals or departures. In all cases, the data volume transmitted by HSDPA users within the past interevent time is subtracted from their remaining data volumes. New HSDPA data rates are calculated, taking the new radio resource and interference situation into account. Finally, the expected departure times of the HSDPA users are updated according to the remaining data volumes and data rates.

7.1. Volume-Based Traffic Model and Spatial Fairness. As mentioned before, an important distinction between QoS and elastic flows is that QoS flows typically follow a time-based traffic model, which means that the user wants to keep the connection a certain time span, for example, for the time of a conversation. In contrast, elastic flows are volume-based, that is, the user leaves the system as soon as a certain data volume is transmitted. In reality, the user behavior is a mixture between both models, depending on factors like user satisfaction, pricing models, type of content. However, the two models can be seen as the extremes of the actual user behavior.

A time-based traffic model implicates that the number of currently active users is independent of the perceived data rates. Moreover, the *spatial distribution* of the number of users is corresponding to the spatial *arrival process*; if users arrive with arrival rate λ, the number of concurrently active users in steady-state follows according to Little as λ/μ, if no blocking occurs.

A volume-based traffic model means that users stay in the system until their service demands are fullfilled. Therefore, the number of active users depends on the assigned data rates. In HSDPA systems, the data rate depends

on the channel quality, which means that users with low average channel qualities stay longer in the system than those with good channel qualities. Since the average channel quality is dominated by the other-cell interference, users at the cell edges stay longer in the system than users in the center of the cell. This implies that the spatial arrival process and the spatial steady state distribution are not directly related anymore, a fact that complicates planning of HSPDA networks significantly. One reason is that Monte Carlo methods [35] now have to estimate the spatial user population for every snapshot, which is difficult without knowledge of the the currently ongoing flows. With round-robin scheduling, a direct formulation of the mean transfer time was found in [5, 24], since in that case the data rates of the users only depend on the number of users and their position, but are otherwise independent of each other.

We now clarify the effect of spatial heterogeneity with some example scenarios. Figure 7 shows the arrival probability and the residency probability versus the distance to the antenna for cell number 2 from the irregular scenario. The arrival probability describes the probability that a user arrives in this cell at a certain point, while the residence probability reflects the spatial distribution of the users in the cell in steady state. The spiky shape of the curves is due to the discretization of the cell area into area elements. It is obvious that arrival and residence probabilities are not equal, and that the magnitude of the deviation depends on the scheduling discipline. MaxTBS scheduling shows the highest deviation, since users close to the antenna leave the system much earlier than users farther away. An interesting result is that residence probabilities with proportional fair scheduling fir slightly better to the arrival probabilities if compared to round-robin scheduling. We will see later that this effect comes from the fact that the proportional fair scheduler favors users on the cell edges.

Figure 8 shows the corresponding ratio between arrival and residence probability in the same cell. With time-based users, the ratio would be equal to one at all distances. With volume-based users and MaxTBS-scheduling, the probability to meet a user at the cell edge is four times higher than the arrival probability at the same location.

The deviation of arrival and residence probabilities is the result of spatial unfairness regarding the data rate allocation. This is demonstrated in Figure 9, which shows the average user throughput depending on the distance to the antenna. MaxTBS-scheduling favors strongly user in the cell center, and thus shows the highest degree of unfairness. Proportional fair and round-robin scheduling lead to more balanced results. The difference between round-robin and proportional fair reflects the scheduling gain due to multiuser diversity. Note that the gain of the proportional fair scheduler over the round-robin scheduler is nearly independent of the distance.

Finally, in Figure 10, the same statistic for the center cell of the homogeneous scenario is shown, but in a scenario with a higher DCH load of $\rho_c = 0.6$. Here, the lack of resources leads to low throughputs, such that the aforementioned favoring of user at the cell edge with proportional fair scheduling is clearly visible. This is caused by the higher variance of the TBS distribution of users which experience more other-cell interference than users close to the antenna, see also [36] for a discussion of this effect.

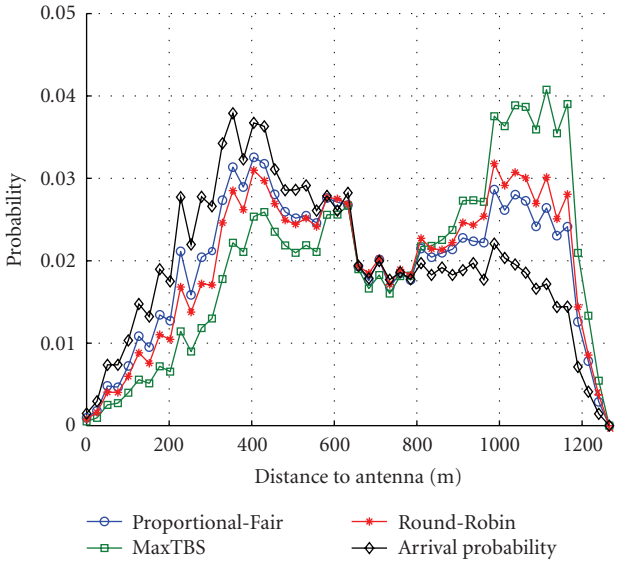

Figure 7: Arrival and residence probabilities for cell 2 in the irregular network with inhomogeneous user arrivals and DCH offered load $\rho_c = 0.4$. The black line with diamond markers indicates the user arrival probability.

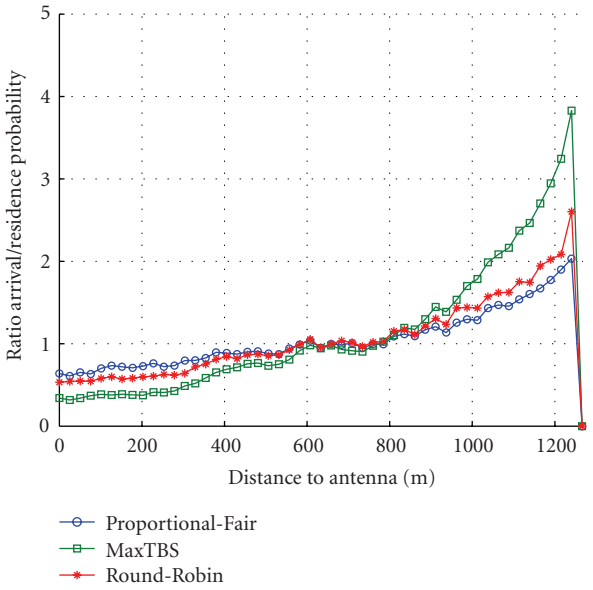

Figure 8: Ratio between arrival and residence probabilities. MaxTBS-scheduling leads to the highest inhomogeneity.

7.2. Impact of Scheduling Disciplines. We now investigate the impact of different scheduling disciplines on the overall performance of the network. We consider the homogeneous scenario with hexagonal cell layout and increase the offered DCH load from 0.1 to 0.8.

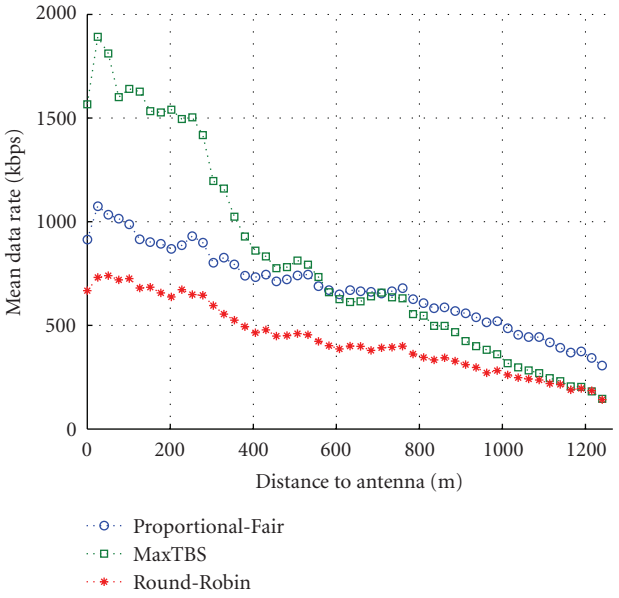

Figure 9: Mean throughput versus distance to antenna with offered DCH load $\rho_c = 0.4$ for cell 2 of the irregular scenario.

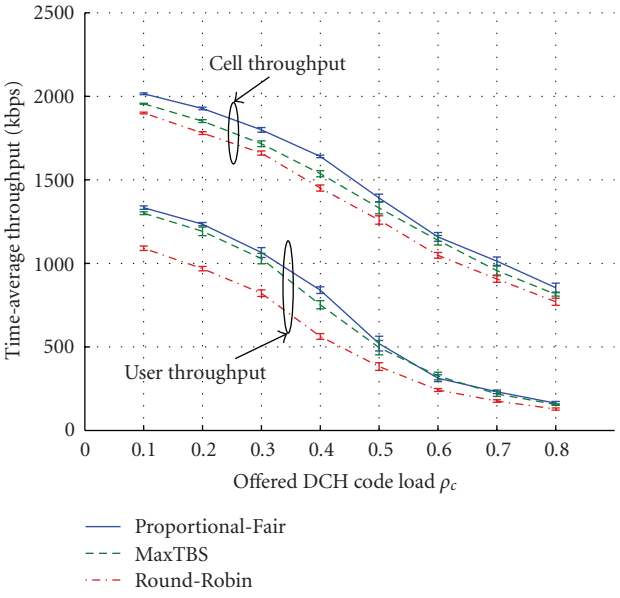

Figure 11: Time-average user and cell throughput versus offered DCH load for different scheduling disciplines.

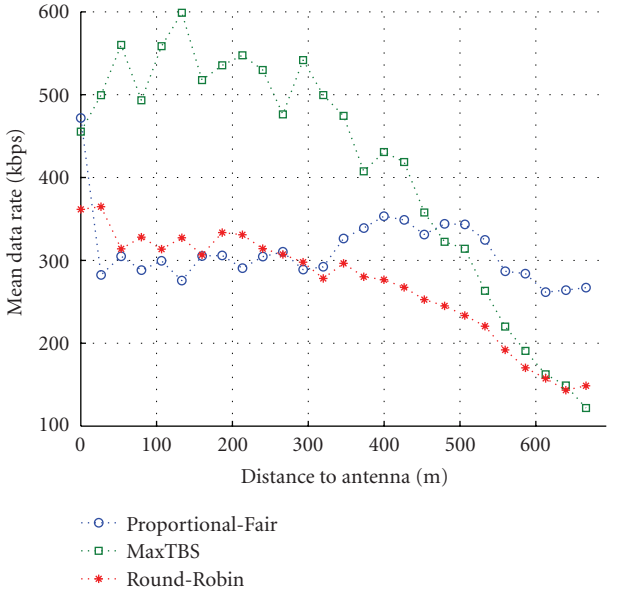

Figure 10: Mean throughput versus distance to antenna for the center cell of the hexagonal scenario with offered DCH load $\rho_c = 0.6$.

Figure 11 shows the resulting time-average cell and user throughput versus the offered DCH load. As expected, the channel-aware scheduling disciplines lead to better results than the channel-blind round-robin discipline, regardless of the DCH load. However, with higher DCH load, the difference between the scheduling disciplines becomes smaller, since the lack of code resources prevents an efficient exploitation of multiuser diversity. An interesting result is that proportional-fair scheduling leads to higher throughput curves than MaxTBS-scheduling, which is at a first glance counter intuitive. MaxTBS-scheduling maximizes cumulated data rates (the sum-rate) for a static scenario, that is, for a fixed number of ongoing flows and consequently also during any interevent time [32]. This also means that MaxTBS-scheduling always leads to a higher cell throughput than proportional-fair scheduling if we consider the same snapshot for both schedulers, reflecting the well known tradeoff between system capacity (defined as cell throughput) and fairness of data rate allocation (see, e.g., [10]).

However, this unfairness means that in cases where the differences between the average channel conditions are large, the MaxTBS scheduler has a strong tendency to overproportionally favor the best user, such that the data rates of the remaining UEs are very low. These users stay very long in the system which is then reflected in the time-average cell and user throughput. With proportional-fair scheduling the data rate of users with good channel conditions is lower, however this is compensated with lower sojourn times of users with bad channel conditions. Note that in principle this also holds for round-robin scheduling, but channel-blindness overweights this effect such that the average throughput is indeed lower.

In the literature, some numerical results seem to contradict the results presented here. In [37, 38], the system throughput for round-robin, proportional fair and Max C/I (i.e., MaxTBS) is shown, and it is concluded that Max C/I scheduling provides the highest average cell throughput. However, the results apply to static scenarios with persistent data flows for a fixed number of users. In such a scenario, MaxTBS scheduling is optimal, but it is not comparable with the flow-level throughput in system with traffic dynamics. In [19], users arrive according to a Poisson process and request 100 KB of data, which is incidentally the same

average amount of data as in our scenario. However, users are dropped from the system if they stay longer than 12.5 seconds in the system, such that the time-average user sojourn time is reduced. So, in fact this study employs a mixture between time-and volume-based traffic model. Consequently, the results show a small performance gain for Max C/I scheduling. Similarly, in [18] users are dropped from the system if their throughput is lower than 9.6 kbps. It is not clear over which time span the throughput is measured, but the dropping of low-bandwidth users skews the time-average throughput to the benefit of the Max C/I scheduler.

Figure 12 shows the CDF of the user and cell throughputs for an offered DCH load of $\rho_c = 0.4$. The CDF of the MaxTBS scheduler confirms the time-average throughput curves; a large portion of the probability weight is on very low data rates, but in the same time the higher quantiles, for example, for 0.8, are higher than for proportional fair and round-robin scheduling. In terms of fairness, it is remarkable that the shape of the curves for Round-robin and proportional-fair are similar with exception of a small peak for low data rates for the proportional fair scheduler. Also note the stair-like shape of cell-throughput CDF for low data rates, which is caused by preemption from DCH connections.

Figure 13 exemplarily demonstrates the behavior of the three schedulers for scenario with three users which have fixed data volumes and Σ-values of -20 dB, -10 dB, and 0 dB. The figure shows the remaining total data volume versus time. Figure 14 shows the corresponding data rates. With MaxTBS scheduling, the first and second users leave the system faster than with the other disciplines (indicated by the vertical dashed lines), but the remaining data volume of the "worst" user with $\Sigma = 0$ dB is so large that in total, the proportional-fair scheduler needs less time to transport the whole data volume. Note that it depends on channel profile and cell layout how large the advantage of the proportional-fair scheduler is and whether it exists at all.

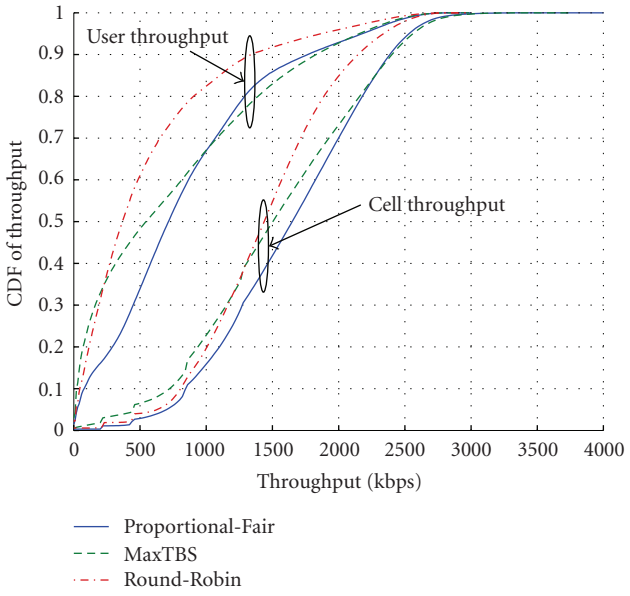

Figure 12: CDF of user and cell throughput for an offered DCH load of $\rho_c = 0.4$.

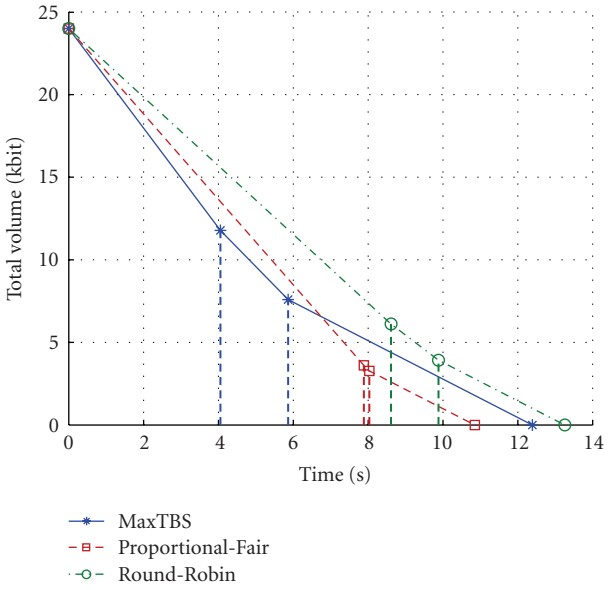

Figure 13: Total remaining data volume versus time for a three-user scenario with fixed data volume. Vertical dashed lines indicate departures.

8. Conclusion and Outlook

We investigated spatial and temporal fairness aspects of integrated HSDPA-enhanced UMTS networks on flow level. Results have been generated with a flow-level simulation which considers the network-wide interference situation and its impact on DCH transmit powers and HSDPA data rates. The latter are calculated with a physical layer abstraction model which considers code resources, multipath-propagation, HS-DSCH transmit power, and different scheduling disciplines.

The numerical results have been generated within two-network scenarios: a homogeneous scenario with hexagonal cells and equal arrival rates over the whole space, and an inhomogeneous scenario with irregular-shaped cells and location-dependent arrival densities. An expected result is that the shared-bandwidth approach of the HSDPA transport channel leads to spatial user residence probabilities which are different to the corresponding arrival probabilities. The degree of unfairness depends on the employed scheduling discipline; "greedy" scheduling disciplines like MaxTBS lead to a high unfairness, while channel-blind round-robin scheduling and proportional fair scheduling show similar results. However, proportional-fair scheduling has a nearly constant relative gain in terms of throughput over round-robin scheduling independent of the distance to the antenna and of the arrival densities.

A further objective of this paper is to understand the flow-level performance of different scheduling disciplines.

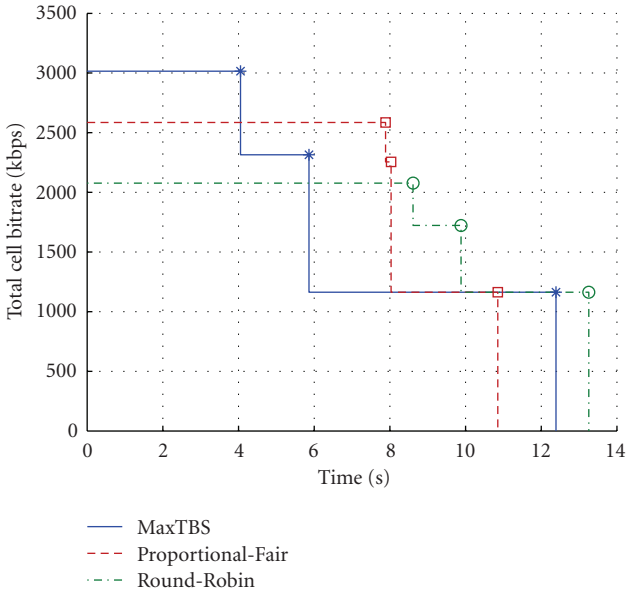

Figure 14: Corresponding cell throughput versus time.

The comparison between round-robin, proportional fair, and MaxTBS scheduling showed that, remarkably, proportional fair scheduling has a slight performance gain in terms of average cell and user throughput. The reason is that although MaxTBS-scheduling maximizes the sum rate within a static scenario, traffic dynamics, and the high unfairness of the data rate allocation with MaxTBS favors in the end proportional fair scheduling. This shows that the consideration of traffic dynamics is a crucial point of the performance evaluation of shared bandwidth systems, and it encourages further investigations of the relation between physical layer parameters and flow-level performance.

References

[1] "Quality of service (QoS) concept and architecture," Tech. Rep. TS 23.107 V6.1.0, 3GPP, Valbonne, France, March 2004.

[2] X. Liu, E. K. P. Chong, and N. B. Shroff, "Optimal opportunistic scheduling in wireless networks," in *Proceedings of the 58th IEEE Vehicular Technology Conference (VTC '03)*, vol. 3, pp. 1417–1421, Orlando, Fla, USA, October 2003.

[3] J. W. Roberts, "A survey on statistical bandwidth sharing," *Computer Networks*, vol. 45, no. 3, pp. 319–332, 2004.

[4] S. Lu, V. Bharghavan, and R. Srikant, "Fair scheduling in wireless packet networks," *IEEE/ACM Transactions on Networking*, vol. 7, no. 4, pp. 473–489, 1999.

[5] R. Litjens, J. van den Berg, and M. Fleuren, "Spatial traffic heterogeneity in HSDPA networks and its impact on network planning," in *Proceedings of the 19th International Teletraffic Congress (ITC '05)*, pp. 653–666, Bejing, China, August-September 2005.

[6] H. van den Berg, R. Litjens, and J. Laverman, "HSDPA flow level performance: the impact of key system and traffic aspects," in *Proceedings of the 7th ACM International Symposium on Modeling, Analysis and Simulation of Wireless and Mobile Systems (MSWiM '04)*, pp. 283–292, Venice, Italy, October 2004.

[7] P. Viswanath, D. N. C. Tse, and R. Laroia, "Opportunistic beamforming using dumb antennas," *IEEE Transactions on Information Theory*, vol. 48, no. 6, pp. 1277–1294, 2002.

[8] X. Liu, E. K. P. Chong, and N. B. Shroff, "A framework for opportunistic scheduling in wireless networks," *Computer Networks*, vol. 41, no. 4, pp. 451–474, 2003.

[9] Y. Liu and E. Knightly, "Opportunistic fair scheduling over multiple wireless channels," in *Proceedings of the 22nd Annual Joint Conference of the IEEE Computer and Communications Societies (INFOCOM '03)*, vol. 2, pp. 1106–1115, San Francisco, Calif, USA, March-April 2003.

[10] L. Yang, M. Kang, and M.-S. Alouini, "On the capacity-fairness tradeoff in multiuser diversity systems," *IEEE Transactions on Vehicular Technology*, vol. 56, no. 4, part 1, pp. 1901–1907, 2007.

[11] R. Knopp and P. A. Humblet, "Information capacity and power control in single-cell multiuser communications," in *Proceedings of IEEE International Conference on Communications (ICC '95)*, vol. 1, pp. 331–335, Seattle, Wash, USA, June 1995.

[12] A. Jalali, R. Padovani, and R. Pankaj, "Data throughput of CDMA-HDR: a high efficiency-high data rate personal communication wireless system," in *Proceedings of the 51st IEEE Vehicular Technology Conference (VTC '00)*, vol. 3, pp. 1854–1858, Tokyo, Japan, May 2000.

[13] P. Ameigeiras, J. Wigard, and P. Mogensen, "Performance of the M-LWDF scheduling algorithm for streaming services in HSDPA," in *Proceedings of the 60th IEEE Vehicular Technology Conference (VTC '04)*, vol. 2, pp. 999–1003, Los Angeles, Calif, USA, September 2004.

[14] M. Lundevall, B. Olin, J. Olsson, et al., "Streaming applications over HSDPA in mixed service scenarios," in *Proceedings of the 60th IEEE Vehicular Technology Conference (VTC '04)*, vol. 2, pp. 841–845, Los Angeles, Calif, USA, September 2004.

[15] A. K. F. Khattab and K. M. F. Elsayed, "Channel-quality dependent earliest deadline due fair scheduling schemes for wireless multimedia networks," in *Proceedings of the 7th ACM International Symposium on Modeling, Analysis and Simulation of Wireless and Mobile Systems (MSWiM '04)*, pp. 31–38, Venice, Italy, October 2004.

[16] M. C. Necker, "A comparison of scheduling mechanisms for service class differentiation in HSDPA networks," *AEU - International Journal of Electronics and Communications*, vol. 60, no. 2, pp. 136–141, 2006.

[17] T. E. Kolding, "QoS-aware proportional fair packet scheduling with required activity detection," in *Proceedings of the 64th IEEE Vehicular Technology Conference (VTC '06)*, pp. 1–5, Montreal, Canada, September 2006.

[18] P. Ameigeiras, J. Wigard, and P. Mogensen, "Performance of packet scheduling methods with different degree of fairness in HSDPA," in *Proceedings of the 60th IEEE Vehicular Technology Conference (VTC '04)*, vol. 2, pp. 860–864, Los Angeles, Calif, USA, September 2004.

[19] T. E. Kolding, F. Frederiksen, and P. E. Mogensen, "Performance aspects of WCDMA systems with high speed downlink packet access (HSDPA)," in *Proceedings of the 56th IEEE Vehicular Technology Conference (VTC '02)*, vol. 1, pp. 477–481, Vancouver, Canada, September 2002.

[20] D. Staehle and A. Mäder, "A model for time-efficient HSDPA simulations," in *Proceedings of the 66th IEEE Vehicular Technology Conference (VTC '07)*, pp. 819–823, Baltimore, Md, USA, September-October 2007.

[21] A. Mäder and D. Staehle, "A flow-level simulation framework for HSDPA-enabled UMTS networks," in *Proceedings of the*

10th ACM Symposium on Modeling, Analysis, and Simulation of Wireless and Mobile Systems (MSWiM '07), pp. 269–278, Chania, Greece, October 2007.

[22] "Medium Access Control (MAC) protocol specification," Tech. Rep. TS 25.321 V6.6.0, 3GPP, Valbonne, France, September 2005.

[23] H. Holma and A. Toskala, Eds., *HSDPA/HSUPA for UMTS: High Speed Radio Access for Mobile Communications*, John Wiley & Sons, New York, NY, USA, 1st edition, 2006.

[24] A. Mäder, D. Staehle, and M. Spahn, "Impact of HSDPA radio resource allocation schemes on the system performance of UMTS networks," in *Proceedings of the 66th IEEE Vehicular Technology Conference (VTC '07)*, pp. 315–319, Baltimore, Md, USA, September-October 2007.

[25] D. Staehle and A. Mäder, "An analytic model for deriving the node-B transmit power in heterogeneous UMTS networks," in *Proceedings of the 59th IEEE Vehicular Technology Conference (VTC '04)*, vol. 4, pp. 2399–2403, Milan, Italy, May 2004.

[26] F. Brouwer, I. de Bruin, J. C. Silva, N. Souto, F. Cercas, and A. Correia, "Usage of link-level performance indicators for HSDPA network-level simulations in E-UMTS," in *Proceedings of the 8th IEEE International Symposium on Spread Spectrum Techniques and Applications (ISSSTA '04)*, pp. 844–848, Sydney, Australia, August-September 2004.

[27] H. J. Kushner and P. A. Whiting, "Convergence of proportional-fair sharing algorithms under general conditions," *IEEE Transactions on Wireless Communications*, vol. 3, no. 4, pp. 1250–1259, 2004.

[28] D. N. Tse, "Optimal power allocation over parallel Gaussian broadcast channels," in *Proceedings of IEEE International Symposium on Information Theory (ISIT '97)*, p. 27, Ulm, Germany, June-July 1997.

[29] L. Li and A. J. Goldsmith, "Capacity and optimal resource allocation for fading broadcast channels—I. Ergodic capacity," *IEEE Transactions on Information Theory*, vol. 47, no. 3, pp. 1083–1102, 2001.

[30] S. Borst, "User-level performance of channel-aware scheduling algorithms in wireless data networks," *IEEE/ACM Transactions on Networking*, vol. 13, no. 3, pp. 636–647, 2005.

[31] U. Türke, M. Koonert, R. Schelb, and C. Görg, "HSDPA performance analysis in UMTS radio network planning simulations," in *Proceedings of the 59th IEEE Vehicular Technology Conference (VTC '04)*, vol. 5, pp. 2555–2559, Milan, Italy, May 2004.

[32] J. M. Holtzman, "CDMA forward link waterfilling power control," in *Proceedings of the 51st IEEE Vehicular Technology Conference (VTC '00)*, vol. 3, pp. 1663–1667, Tokyo, Japan, May 2000.

[33] A. Furuskär, S. Parkvall, M. Persson, and M. Samuelsson, "Performance of WCDMA high speed packet data," in *Proceedings of the 55th IEEE Vehicular Technology Conference (VTC '02)*, vol. 3, pp. 1116–1120, Birmingham, Ala, USA, May 2002.

[34] A. Haider, R. Harris, and H. Sirisena, "Simulation-based performance analysis of HSDPA for UMTS networks," in *Proceedings of the Australian Telecommunication Networks and Applications Conference (ATNAC '06)*, Melbourne, Australia, December 2006.

[35] U. Türke, M. Koonert, R. Schelb, and C. Görg, "HSDPA performance analysis in UMTS radio network planning simulations," in *Proceedings of the 59th IEEE Vehicular Technology Conference (VTC '04)*, vol. 5, pp. 2555–2559, Milan, Italy, May 2004.

[36] J. M. Holtzman, "CDMA forward link waterfilling power control," in *Proceedings of the 51st IEEE Vehicular Technology Conference (VTC '00)*, vol. 3, pp. 1663–1667, Tokyo, Japan, May 2000.

[37] A. Furuskär, S. Parkvall, M. Persson, and M. Samuelsson, "Performance of WCDMA high speed packet data," in *Proceedings of the 55th IEEE Vehicular Technology Conference (VTC '02)*, vol. 3, pp. 1116–1120, Birmingham, Ala, USA, May 2002.

[38] A. Haider, R. Harris, and H. Sirisena, "Simulation-based performance analysis of HSDPA for UMTS networks," in *Proceedings of the Australian Telecommunication Networks and Applications Conference (ATNAC '06)*, Melbourne, Australia, December 2006.

EURASIP Journal on Advances in Signal Processing

Special Issue on
Filter Banks for Next-Generation Multicarrier Wireless Communications

Call for Papers

Digital filter banks find various good applications in communications signal processing. In general, they can be used to obtain very sharp frequency selectivity to isolate different communications frequency channels from each other and from interfering spectral components. This can be done in a very flexible and dynamic manner. Thus, filter banks constitute a very powerful generic tool for software-defined radios and spectrally agile communication systems.

The theoretical capacity limits in communications can be approached by multicarrier techniques. With radio channels, multicarrier techniques can be combined with multiantenna transmitters and receivers to provide efficiency. Existing or planned transmission systems rely on the OFDM technique to reach these goals. However, OFDM has a number of drawbacks, such as the use of the cyclic prefix to cope with the channel impulse response which results in a loss of capacity and the requirement of block processing to maintain orthogonality among all the subcarriers. Furthermore, the leakage among frequency subbands has a serious impact on the performance of FFT-based spectrum sensing and OFDM-based cognitive radio in general.

So far, some attempts have been made to introduce filter bank multicarrier (FBMC) in the radio communications arena, in particular, the isotropic orthogonal transform algorithm (IOTA). However, the full exploitation and optimization of FBMC techniques in the context of radio evolution have not been considered sufficiently. Consequently, advances in communication aspects of FBMC are still required to make it useful for future radio systems.

This has motivated advanced research in the European ICT project PHYDYAS, which supports this special issue. Topics of interest include, but are not limited to:

- Filter bank-based multicarrier transmission and prototype filter design
- Filter bank-based signal processing for other communication waveforms
- Filter bank applications in software-defined radio
- Data-aided and blind techniques for synchronization and channel estimation
- Preamble and pilot-pattern design
- Equalization and demodulation
- FBMC MIMO techniques and beamforming
- Radio scene spectrum analysis and cognitive radio
- Interference management
- Interlayer optimization and FBMC-specific scheduling
- Filter bank for channel coding
- Filter bank in AD and DA conversions

Before submission authors should carefully read over the journal's Author Guidelines, which are located at http://www.hindawi.com/journals/asp/guidelines.html. Prospective authors should submit an electronic copy of their complete manuscript through the journal Manuscript Tracking System at http://mts.hindawi.com/, according to the following timetable:

Manuscript Due	June 1, 2009
First Round of Reviews	September 1, 2009
Publication Date	December 1, 2009

Lead Guest Editor

Markku Renfors, Department of Communications Engineering, Tampere University of Technology (TUT), 33720 Tampere, Finland; markku.renfors@tut.fi

Guest Editors

Pierre Siohan, Orange Labs 4, France Telécom, rue du Clos Courtel, BP 91226, 35512 Cesson Sévigné Cedex, France; pierre.siohan@orange-ftgroup.com

Behrouz Farhang-Boroujeny, Department of Electrical and Computer Engineering, University of Utah, 3280 MEB Salt Lake City, UT 84112, USA; farhang@ece.utah.edu

Faouzi Bader, Centre Tecnologic de Telecommunication de Catalunya (CTTC), Parc Mediterrani de la Tecnologia, Avenue Canal Olimpic, Casstelldefels, 08860 Barcelona, Spain; faouzi.bader@cttc.es

EURASIP Journal on Embedded Systems

Special Issue on
Design Methodologies and Innovative Architectures for Mixed-Signal Embedded Systems

Call for Papers

The continuous evolution of CMOS technologies, and its variants HV MOS, BCD, and RF CMOS, has enabled the integration of complex functionalities in a single heterogeneous embedded system. Digital subsystems can be integrated onto the same chip or the same package together with RF blocks, analog circuits, power drivers, and even micromechanical parts for sensors and actuators. Such new generation of mixed-signal embedded systems is fueling the development of more efficient and performing solutions in several technology areas: sensors, lab-on-chip, and body area networks for health care; distributed control sensing actuation units for increasing safety, comfort, and engine efficiency in vehicles; software-defined and cognitive radios for multimode multimedia communication; wireless sensor/actuator networks for ambient intelligence.

The opportunity given by mixed-signal embedded systems comes with lots of challenges. The main issues concern the development of innovative methods, languages, CAD tools, and architectures needed in different design phases: high-level specification and simulation, design space exploration to find optimal partitioning between hardware/software and analog/digital functions; codesign of the different subsystems; automatic synthesis; design flexibility and programmability, IP block reuse, and on field reconfigurability; verification and test of mixed-signal components by means of simulations, formal methods, and rapid prototyping; assembly and integration of heterogeneous blocks in the same chip or package.

This Special Issue intends to also address case studies, in the above-mentioned technology areas, demonstrating how the use of mixed-signal embedded systems enables new services/applications or increases the performance and efficiency of existing ones. Authors working in the area of mixed-signal embedded systems are requested to submit original papers or high-quality review articles addressing recent advances in the field. If the work has been published in conference proceedings, the authors should submit an extended version. The topics include, but are not limited to:

- High-performance ADCs and DACs
- Digital calibration/correction of analog and RF circuits in embedded systems with wireless connectivity
- Integration of MEMS, analog, and digital circuits in smart embedded sensors
- Digital and power integration for smart actuators
- Methods for the design of space exploration of mixed-signal architectures and partitioning between hardware/software and analog/digital domains
- CAD tools and languages for mixed-signal embedded systems
- Rapid prototyping techniques and test beds for mixed-signal embedded systems
- Application case studies

Before submission, authors should carefully read over the journal's Author Guidelines, which are located at http://www.hindawi.com/journals/es/guidelines.html. Prospective authors should submit an electronic copy of their complete manuscript through the journal Manuscript Tracking System at http://mts.hindawi.com/ according to the following timetable:

Manuscript Due	June 1, 2009
First Round of Reviews	September 1, 2009
Publication Date	December 1, 2009

Lead Guest Editor

Sergio Saponara, Università di Pisa, Via G. Caruso 16, 56122 Pisa, Italy; sergio.saponara@iet.unipi.it

Guest Editors

Pierluigi Nuzzo, University of California at Berkeley, 205 Cory Hall, Berkeley, CA 94720, USA; nuzzo@eecs.berkeley.edu

Paolo D'Abramo, Austriamicrosystems AG, Schloss Premstaetten, Austria; paolo.dabramo@austriamicrosystems.com

Luca Fanucci, Università di Pisa, Via G. Caruso 16, 56122 Pisa, Italy; luca.fanucci@iet.unipi.it